



HAL
open science

SUMO-modified nuclear cyclin D1 bypasses Ras-induced senescence

Xin Lu, Xiaodan Wang, Eleonora Lapi, Alexandra Sullivan, Indrika Ratnayaka, Robert Goldin, Ronald Hay

► **To cite this version:**

Xin Lu, Xiaodan Wang, Eleonora Lapi, Alexandra Sullivan, Indrika Ratnayaka, et al. SUMO-modified nuclear cyclin D1 bypasses Ras-induced senescence. *Cell Death and Differentiation*, 2010, 10.1038/cdd.2010.101 . hal-00570132

HAL Id: hal-00570132

<https://hal.science/hal-00570132>

Submitted on 27 Feb 2011

HAL is a multi-disciplinary open access archive for the deposit and dissemination of scientific research documents, whether they are published or not. The documents may come from teaching and research institutions in France or abroad, or from public or private research centers.

L'archive ouverte pluridisciplinaire **HAL**, est destinée au dépôt et à la diffusion de documents scientifiques de niveau recherche, publiés ou non, émanant des établissements d'enseignement et de recherche français ou étrangers, des laboratoires publics ou privés.

SUMO-modified nuclear cyclin D1 bypasses Ras-induced senescence

Running title: ASPP2 regulates nuclear localisation of cyclin D1

Xiao Dan Wang^{1^}, Eleonora Lapi^{1^}, Alexandra Sullivan^{1,4}, Indrika Ratnayaka¹, Robert Goldin², Ronald Hay³ and Xin Lu^{1*}

(1) Ludwig Institute for Cancer Research, Nuffield Department of Clinical Medicine, University of Oxford, Oxford OX3 7DQ, United Kingdom.

(2) Department of Pathology, Imperial College London, Faculty of Medicine at St. Mary's, Norfolk Place, London W2 1PG, United Kingdom.

(3) Wellcome Trust Centre for Gene Regulation and Expression, College of Life Sciences, University of Dundee, Dundee DD1 5EH, United Kingdom.

(4) Present address: Centre for Cell Signalling, Institute of Cancer, Barts and the London School of Medicine and Dentistry, Charterhouse Square, London EC1M 6BQ, United Kingdom.

[^] These authors contributed equally

**Corresponding author*

Tel: 44 (0)1865 617500

Fax: 44 (0)1865 617515

E-mail: xin.lu@ludwig.ox.ac.uk

Abstract

Oncogene-induced senescence represents a key tumour suppressive mechanism. Here we show that Ras oncogene-induced senescence can be mediated by the recently identified haploinsufficient tumour suppressor ASPP2 through a novel and p53/p19^{Arf}/p21^{waf1/cip1}-independent pathway. ASPP2 suppresses Ras-induced SUMO-modified nuclear cyclin D1 and inhibits Rb phosphorylation. The lysine residue K33 of cyclin D1 is a key site for this newly identified regulation. In agreement with the fact that its nuclear localisation is required for its oncogenic activity, we show that nuclear cyclin D1 is far more potent than wild type cyclin D1 in bypassing Ras-induced senescence. Thus, this study identifies SUMO modification as a positive regulator of nuclear cyclin D1, and reveals a new way by which cell cycle entry and senescence are regulated.

Introduction

Cellular senescence is an irreversible cell cycle arrest and is one of the major cellular processes that suppress tumour growth. Cyclin dependent kinases (CDKs) represent one of the main regulators of cellular senescence. This is predominantly achieved through their ability to phosphorylate the retinoblastoma protein Rb, and to prevent Rb from binding and inhibiting E2F, a family of transcription factors that control the expression of essential genes for cell cycle progression. Consistent with their essential role in controlling proliferation, deregulation of the CDK pathways is a common event in various human cancers. Amplification and over-expression of cyclin D1, a regulatory subunit of cdk4/cdk6, has been observed in around 50% of human breast and oesophageal cancers (1, 2). Interestingly, however, elevation of cyclin D1 protein alone is not sufficient to induce tumour growth *in vivo* (3, 4). This is partly due to the fact that cyclin D1/CDK4 or cyclin D1/cdk6 complexes shuttle between nuclear and cytoplasmic compartments during cell cycle progression (5, 6). Additionally, the cyclin D1/cdk4 or cyclin D1/cdk6 complex needs to locate in the nucleus to phosphorylate Rb during S-phase in order to promote cell proliferation. Nuclear export, coupled with ubiquitin-dependent destruction of cyclin D1 in the cytoplasm during S-phase, is one of the best known mechanisms that effectively controls the kinase activity of cyclin D1/cdk4. Hence, nuclear accumulation of cyclin D1 may be one of the main mechanisms by which cyclin D1 exert its oncogenic effects. In agreement with this, overexpression of a mutant cyclin D1 (D1T286A), which is defective in phosphorylation-mediated nuclear export and subsequent proteolysis, induces cell transformation *in vitro* and triggers B-cell lymphoma *in vivo* (6, 7). Furthermore, transgenic mice that over-express the identical mutant cyclin D1 driven by MMTV promoter (MMTV-D1T286A) developed mammary

adenocarcinoma with a shorter latency relative to mice over-expressing the wild type cyclin D1 (MMTV-D1) (8). These observations support the notion that the subcellular localisation of cyclin D1 is critical in controlling its tumourigenicity. Identifying the molecular mechanisms that regulate the nuclear localisation of cyclin D1 is, therefore, vital for our understanding of tumour development and therapy.

SUMOylation is a form of post-translational modification that is known to regulate the cellular localisation of modified proteins (9). Small ubiquitin-related modifiers (SUMOs) are ubiquitin-like polypeptides that become covalently conjugated to cellular proteins in a manner similar to ubiquitylation (9). In vertebrates, three SUMO isoforms are expressed. SUMO-1 shares 43% identity with SUMO-2 and SUMO-3, whereas the latter two are closely related (sharing 97% identity) (10). There are several differences between the mammalian SUMO paralogues, most importantly the overall cellular concentration of SUMO-2/3 is greater than that of SUMO-1, as is the pool of free protein available for conjugation (11). Additionally, they have a different pattern of conjugation: SUMO-2 and SUMO-3 can form conjugated chains through a single conserved acceptor lysine (12, 13), while SUMO-1 does not have an equivalent lysine residue, and thus probably does not act as a link in elongating chains *in vivo*. However, it is possible that SUMO-1 may terminate chains that are elongated through serial conjugation of SUMO-2/3 (14). The conjugation process involves an enzymatic cascade comprising the E1-activating enzyme Aos1 (also known as Uba2 and Sae1), the E2-conjugating enzyme Ubc9 and E3 ligases, including the PIAS family members RanBP2 and hPC2 (9, 15).

Oncogenic stress is one of the best studied cellular senescence-inducing signals and, of the oncogenes identified to date, Ras is the prototype. The Ras oncogene has been shown to predominantly use either p16^{ink4a}/Rb or the Arf/p21^{waf1/cip1}/p53 pathway to mediate cellular senescence. By inducing p16^{ink4a} expression, the Ras oncogene prevents cyclin dependent kinase from phosphorylating Rb. As a result, the de-phosphorylated Rb prevents cell cycle entry by binding and inhibiting the transcriptional activity of E2F. Perhaps one of the most well studied pathways is that by which Ras oncogene induces cellular senescence via the Arf/p21^{waf1/cip1}/p53 pathway. Once Ras induces Arf expression, Arf can bind mdm2 and prevent it from targeting p53 for proteosomal degradation. In turn, the induced p53 transactivates its target genes such as p21^{waf1/cip1}, which can then inhibit cyclin dependent kinases (CDKs) and inhibit cell growth (16-19). However, it is now becoming clear that Ras oncogene can also induce senescence via p53 independent pathways such as C/EBPbeta, or via p63 mediated pathways (20, 21).

ASPP2 belongs to the evolutionarily conserved ASPP family of proteins that were initially identified through their ability to bind to, and regulate, the apoptotic function of p53 and its family members p63 and p73 (ref Daniele) (22). Two different ASPP2 transgenic mouse models were generated and they express either exon 3 or exons 10-17 deleted ASPP2 genes. To differentiate between these two mouse models, they will be referred to here as ASPP2^(Δ3/ Δ3) and ASPP2^(Δ10-17/ Δ10-17) respectively. Importantly, heterozygous mice of ASPP2^(Δ3/ +) and ASPP2^(Δ10-17) are both prone to developing spontaneous tumours, establishing ASPP2 as a new haploinsufficient tumour suppressor (23) (24). The tumour suppressive function of ASPP2 is further supported by the observations that ASPP2 expression is frequently down regulated in human tumours, and reduced ASPP2 expression is tightly associated with patients'

poor prognosis (25, 26). Since ASPP2 can bind other cellular proteins including p65RelA, Bcl2, protein phosphatase 1 (PP1), YAP, APCL and APP-BP1 (27-32), it is possible that ASPP2 may suppress tumour growth in ways other than promoting p53 mediated apoptosis. Since apoptosis and senescence are two major cellular processes that suppress tumour growth, we thus investigated whether ASPP2 can exert its tumour suppressive effects by mediating cellular senescence.

Here we show that Ras oncogene-induced senescence can be mediated by ASPP2. This is achieved through its ability to prevent Ras oncogene from inducing nuclear accumulated cyclin D1. Importantly, ASPP2 mutant cells allowed us to identify SUMO modification as a novel regulation that leads to nuclear localisation of cyclin D1. K33 of cyclin D1 is predominantly responsible for this newly identified modification. Nuclear localisation is vital for the oncogenic properties of cyclin D1 *in vitro* and *in vivo*, and this is supported by the observation that nuclear cyclin D1 is able to bypass Ras-induced senescence.

Results

H-RasV12-induced senescence is mediated by ASPP2

Mouse embryonic fibroblasts (MEFs) are a well established experimental system with which to study oncogene-induced senescence. To investigate whether ASPP2 plays a role in mediating Ras oncogene induced senescence, MEFs were generated from ASPP2^(+/+) and ASPP2^(Δ3/Δ3) embryos, where exon 3 of the murine ASPP2 gene was deleted as previously described (23), and infected with oncogenic H-RasV12. As expected, the expression of oncogenic H-RasV12-induced senescence

in ASPP2^(+/+) MEFs was detected by the presence of the senescence marker SA- β -Gal, but not in ASPP2^(Δ 3/ Δ 3) MEFs (Fig. 1A, B).

The ability of ASPP2 to suppress the transforming activity of H-RasV12 was further investigated using a soft agar assay to measure anchorage independence. While ASPP2^(Δ 3/ Δ 3) MEFs formed few small soft agar colonies, H-RasV12-expressing ASPP2^(Δ 3/ Δ 3) MEFs formed at least ten times more and bigger colonies than those seen in ASPP2^(+/+) MEFs (Fig. 1C). Retroviruses expressing full length ASPP2 were used to infect H-RasV12-expressing ASPP2^(Δ 3/ Δ 3) MEFs, to investigate whether the reintroduction of ASPP2 could mediate H-RasV12-induced senescence. SA- β -Gal activity was detected in around 30% of the cells infected with retroviruses expressing ASPP2 (Fig. 1D). In MEFs, Ras-induced cellular senescence is the predominant phenomenon. p53 also predominantly induces senescence rather than apoptosis in Ras-expressing MEFs. In agreement with this, we also failed to detect any impact of ASPP2 in inducing apoptosis (data not shown). These results illustrate that ASPP2 is a novel mediator of H-RasV12-induced senescence. ASPP2 prevents H-RasV12 from transforming MEFs by mediating H-RasV12-induced senescence.

ASPP2 mediates Ras-induced senescence by preventing H-RasV12-induced nuclear accumulation of cyclin D1

Since Ras oncogene can induce senescence through a p53-dependent pathway and ASPP2 was originally identified as an activator of p53, we checked whether ASPP2 could affect H-RasV12-induced expression of p19^{Arf}, p53 and p21^{waf1/cip1}. Interestingly, the expression of H-RasV12 caused a similar increase in the expression levels of p19^{Arf}, p53 and p21^{waf1/cip1} in both ASPP2^(+/+) and ASPP2^(Δ 3/ Δ 3) MEFs (Fig.

2A). These results suggest that ASPP2 is likely to mediate Ras oncogene-induced senescence independently of p53.

The tumour suppressor Rb represents another cellular senescence pathway. To examine whether ASPP2 mediates Ras oncogene-induced senescence through the Rb pathway, we first compared the phosphorylation status of Rb in ASPP2^(+/+) and ASPP2^(Δ3/Δ3) MEFs. As shown in figure 2B, similar amounts of phosphorylated Rb were detected in both ASPP2^(+/+) and ASPP2^(Δ3/Δ3) MEFs. Interestingly, Ras oncogene only induced a clear reduction of Rb phosphorylation in ASPP2^(+/+) MEFs, whereas it caused a marked 3-4 fold increase in the amount of phosphorylated Rb in H-RasV12 expressing ASPP2^(Δ3/Δ3) MEFs (Fig. 2B). These results suggest that ASPP2 is required for the Ras oncogene to inhibit Rb phosphorylation, and ASPP2 may use this property to mediate Ras oncogene-induced senescence.

To understand how H-RasV12 affects Rb phosphorylation in the absence of functional ASPP2, we investigated the expression levels of cyclin dependent kinases and their inhibitors in ASPP2^(+/+) and ASPP2^(Δ3/Δ3) MEFs, with or without H-RasV12 infection. We observed that the expression levels of cdk4, p16^{ink4a}, p27kip1, cyclin E, cyclin A and cdk2 are not affected by ASPP2 status (Fig. 2C). Interestingly, however, ASPP2 status does affect the expression pattern of cyclin D1. Although cyclin D1 protein levels were increased in both H-RasV12-expressing ASPP2^(+/+) and ASPP2^(Δ3/Δ3) MEFs, increased cyclin D1 was often associated with expression of higher molecular weight (MW) protein bands in H-RasV12 expressing ASPP2^(Δ3/Δ3) MEFs, detected by at least two different anti-cyclin D1 antibodies (Fig. 2C and data not shown). This suggests that ASPP2 may mediate the post-translational modification of cyclin D1 induced by Ras oncogene. It is important to note that we failed to detect similar changes in p53^(+/+) and p53^(-/-) MEFs, irrespective of Ras expression (Fig. 2D). Hence only ASPP2, but not p53, may influence cyclin D1 expression in response to Ras oncogene. Since cyclin D1 is a regulatory subunit of

CDKs, this observation suggests that modified cyclin D1 may be responsible for the observed increase in Rb phosphorylation.

Nuclear localisation is critical for cyclin D1 to form an active complex with CDK4/CDK6 and to phosphorylate Rb. It has also been reported that only nuclear cyclin D1 confers tumour growth (33). Remarkably, ASPP2^(Δ3/Δ3) MEFs had a prominent, 4-fold higher number of nuclear cyclin D1-expressing cells in response to H-RasV12 induction in comparison to that found in ASPP2^(+/+) MEFs (Fig. 2E). In contrast, no difference was observed in the nuclear localisation of p21^{waf1/cip1} between ASPP2^(+/+) and ASPP2^(Δ3/Δ3) MEFs (Suppl.Fig. 1). Furthermore, H-RasV12-induced nuclear accumulation of cyclin D1 was specifically prevented by ASPP2, but not by p53, since similar numbers of nuclear cyclin D1 were detected in Ras-expressing p53^(+/+) and p53^(-/-) MEFs (Fig. 2E, middle panel). This confirms that the pathway regulated by Ras and ASPP2 is p53-independent. Together, the results show that ASPP2 mediates H-RasV12-induced senescence by preventing H-RasV12 from inducing nuclear cyclin D1, Rb phosphorylation and cell cycle entry.

H-RasV12 induces SUMOylation of cyclin D1

Due to the large change in gel mobility, we hypothesised that cyclin D1 modification was likely caused by molecules that can form large chains, such as those formed by poly-ubiquitylation, SUMOylation or a combination of both. Cyclin D1 is known to be ubiquitinated and Ras may influence its ubiquitination (34). We, therefore, first tested whether the presence of H-RasV12 can influence the expression pattern of ubiquitinated cyclin D1 in ASPP2^(Δ3/Δ3) cells. The high MW cyclin D1 observed in figure 2C was highly insoluble and only detected when 8M urea buffer was used to lyse the cells. Thus, 8M urea cell lysates were first diluted 10-fold in NP-

40 buffer to refold the solubilised and denatured high molecular weight cyclin D1, in order to allow an anti-cyclin D1 antibody to specifically immunoprecipitate cyclin D1. The presence of ubiquitinated cyclin D1 was analysed using an anti-ubiquitin antibody. Ubiquitinated protein was enriched by treating the cells with the proteasome inhibitor MG132. Interestingly, H-RasV12 expression did not significantly alter the expression pattern of ubiquitinated proteins in ASPP2^(Δ3/Δ3) cells (Fig. 3A, lanes 1-4). Furthermore, the ubiquitinated cyclin D1 expression pattern detected from cyclin D1 immunoprecipitates was similar between vector or H-RasV12 expressing ASPP2^(Δ3/Δ3) cells (Fig 3A, lanes 5 and 6). Treatment with MG132 also had a minimal impact on the expression pattern of ubiquitinated cyclin D1 (Fig 3A, Lanes 8 and 9). Importantly, the ubiquitinated cyclin D1 had a completely different mobility pattern to that observed in figure 2C, suggesting that the high mobility cyclin D1 bands detected in H-RasV12-expressing ASPP2^(Δ3/Δ3) cells were unlikely to be caused by altered ubiquitination activity in these cells.

SUMO modification, in particular by SUMO2 and SUMO3, is known to often alter a protein's cellular localisation. Knowing that modified cyclin D1 is tightly associated with the accumulation of nuclear cyclin D1, we tested whether cyclin D1 could be SUMO-modified, and whether this modification was altered in H-RasV12-expressing ASPP2^(Δ3/Δ3) cells. Interestingly, we detected an enrichment of SUMO2/SUMO3 modified protein in H-RasV12 expressing ASPP2^(Δ3/Δ3) cells, in comparison to ASPP2^(Δ3/Δ3) cells expressing vector only (Fig. 3B, compare lanes 1 and 2). We also detected a distinct expression pattern of high MW bands in cyclin D1 immunoprecipitates derived from H-RasV12 expressing ASPP2^(Δ3/Δ3) MEFs in comparison to vector only expressing ASPP2^(Δ3/Δ3) MEFs (Fig. 3B, lanes 3 and 4). In particular, we detected an enrichment of SUMO-modified cyclin D1 with molecular

weights ranging from 35Kd to 50Kd (labelled band 2 and 3 for example). These results suggest that cyclin D1 may be SUMO-modified, and that H-RasV12 enhances this modification in ASPP2^(Δ3/Δ3) MEFs.

To provide further evidence that cyclin D1 can be SUMO-modified, we co-transfected His-tagged SUMO-expressing plasmids together with cyclin D1 into ASPP2^(Δ3/Δ3) MEFs, with or without H-RasV12. Expressed His-tagged SUMO was pulled down by nickel beads and the presence of cyclin D1 was detected by an anti-cyclin D1 antibody. Under the experimental conditions used, the nickel beads pulled down co-transfected cyclin D1 non-specifically (Fig. 3C, lanes 1 and 2). However, when co-transfected with SUMO1, the nickel beads pulled down more cyclin D1. Most importantly, they pulled down high molecular weight cyclin D1, similar to that seen in figure 3B. Furthermore, the presence of H-RasV12 enriched the amount of SUMO-modified cyclin D1 (Fig. 3C, lanes 3 and 4, in particular band 3 in lane 4). The number of high MW cyclin D1 was further increased when SUMO1-3 were co-expressed with cyclin D1 (Fig. 3C, lanes 5 and 6, in particular bands 2 and 3 in lane 6). The pattern of high MW cyclin D1 resembled that detected by probing immunoprecipitated endogenous cyclin D1 with anti-SUMO antibody. These results illustrate that cyclin D1 is SUMO-modified, and that this modification is induced by H-RasV12 in ASPP2^(Δ3/Δ3) MEFs.

SUMO modification leads to nuclear accumulation of cyclin D1

SUMO modification is often associated with the specific cellular localisation of modified proteins. Thus, we checked the localisation of exogenously expressed

cyclin D1 in a human osteosarcoma cell line (U2OS), that express endogenous Ras and ASPP2, in the presence of SUMO-1, SUMO-2 and SUMO-3 expressing plasmids. Interestingly, nuclear cyclin D1 was detected in more than 60% of U2OS cells co-expressing cyclin D1 and SUMO-2 and 3 (but not SUMO-1)(Fig. 4A). To confirm the role of SUMOylation in the nuclear localisation of cyclin D1, we infected H-RasV12-expressing ASPP2^(Δ3/Δ3) MEFs with adenovirus-expressing SENP2, a protease that specifically removes SUMO modifications. We observed that nuclear cyclin D1 disappeared from cells infected by SENP2-expressing adenovirus, but not from cells infected by control virus, (Fig. 4B), suggesting that SUMO modification is required for the accumulation of nuclear cyclin D1.

SUMO modification on lysine 33 is critical for the nuclear localisation of cyclin D1

Sequence analysis performed with the SUMOsp web server (35) revealed the existence of 4 putative SUMOylation sites on cyclin D1: a canonical one at K33 (lysine 33), and 3 type II sites at K72, K95 and K96 (Fig. 5A). To identify the lysine residue important for cyclin D1 modification and nuclear localisation, residues K33, K72, K95 and K96 were individually mutated to alanine (A) to generate non-modifiable cyclin D1 mutants K33A, K72A, K95A and K96A respectively. The cellular localisations of exogenously expressed cyclin D1 and its mutants in the presence of SUMO-2 and SUMO-3 expressing plasmids (Fig. 5B) were then examined. Interestingly, nuclear cyclin D1 was detected in 60-70% of the cells co-expressing cyclin D1, cyclin D1-K72A, cyclin D1-K95A and cyclin D1-K96A with SUMO-2 and 3, but only in 15% of the cells co-expressing cyclin D1-K33A and SUMO-2 and -3. These results demonstrate that SUMO is likely to modify cyclin D1 on K33, and that K33 is a residue that is critical for cyclin D1's nuclear localisation.

Nuclear cyclin D1 is more potent than wild type cyclin D1 in rescuing Ras-induced senescence

Cyclin D1 is phosphorylated by GSK-3 β on a conserved C-terminal threonine, Thr-286, during the G1/S transition (5). CRM1 binds Thr-286 phosphorylated cyclin D1 in the nucleus and exports it to the cytoplasm. Once in the cytoplasm, Thr-286 phosphorylated cyclin D1 is ubiquitinated and targeted for proteasome-mediated degradation. Thus, by mutating Thr-286 to Ala-286, the resulting mutant cyclin D1 T286A is refractory to GSK-3 β -dependent phosphorylation and CRM export, so is constitutively nuclear. Importantly, transgenic mouse model studies have shown that the nuclear cyclin D1 T286A mutant, but not wild type cyclin D1, has the oncogenic potential to promote cell transformation *in vitro* and tumour growth in nude mice when overexpressed (3, 4, 6, 36).

Knowing that H-RasV12-induced nuclear accumulation of cyclin D1 fails to induce cellular senescence in ASPP2^(Δ 3/ Δ 3) MEFs, we hypothesised that ASPP2 mediates H-RasV12-induced senescence by preventing the nuclear accumulation of cyclin D1. Cyclin D1 is, therefore, a downstream effector of ASPP2, and nuclear cyclin D1 should be able to bypass H-RasV12-induced senescence in ASPP2^(+/+) MEFs. ASPP2^(+/+) MEFs were infected with oncogenic H-RasV12 alone, or in combination with cyclin D1 or cyclin D1 T286A. Protein expression levels and cellular localisation of WT and cyclin D1 T286A were then examined via immunoblotting and immunofluorescence staining (Fig. 6A and 6B). The expression of oncogenic H-RasV12 was found to induce endogenous cyclin D1 expression (Fig. 6A, compare lanes 1 and 4). This induction was at the mRNA level ((37) and data not shown) and agreed with previous findings. However, H-RasV12 expression did not affect exogenously expressed cyclin D1 or cyclin D1 T286A (Fig. 6A, compare lanes 2 and 5 and lanes 3 and 6), allowing us to test whether nuclear cyclin D1 was more potent than WT cyclin D1 in bypassing H-RasV12-induced senescence.

ASPP2^(+/+) MEFs were infected by H-RasV12 alone, or in combination with either WT cyclin D1 or nuclear mutant cyclin D1 T286A, as indicated. Seven days later, SA-β-Gal staining or 24 hour BrdU labelling was used to identify senescent cells. The results shown in figure 6C and 6E show that very few ASPP2^(+/+) MEFs underwent senescence when infected with retroviruses expressing either cyclin D1 or cyclin D1 T286A. Under the same conditions, however, around 90% of the cells infected with H-RasV12 alone stained positive for SA-β-Gal. When cells were co-infected with H-RasV12 and WT cyclin D1, the number of SA-β-Gal positive cells reduced to around 65%. Perhaps most importantly, when H-RasV12 was co-infected with nuclear cyclin D1 T286A, only 25% of the cells stained positive for SA-β-Gal. Interestingly, the SA-β-Gal staining pattern was almost a mirror image of that of BrdU-labelled cells. Around 80% of cyclin D1 or cyclin D1 T286-infected ASPP2^(+/+) MEFs were positive for BrdU, whereas less than 10% of H-RasV12 expressing ASPP2^(+/+) MEFs were labelled BrdU-positive. Furthermore, while only 20% of BrdU-positive cells were detected in ASPP2^(+/+) MEFs co-infected with H-RasV12 and cyclin D1, 60% of cells detected in ASPP2^(+/+) MEFs co-infected with H-RasV12 and cyclin D1 T286A were BrdU-positive (Fig. 6D and 6F). These results demonstrate that nuclear cyclin D1 is more potent than wild type cyclin D1 in bypassing Ras oncogene-induced cellular senescence.

Discussion

By investigating the mechanisms that ASPP2 uses to mediate Ras oncogene-induced senescence, we identified SUMOylation as a novel mechanism that regulates the nuclear localisation of cyclin D1. We also showed that nuclear cyclin D1 is more effective than wild type cyclin D1 in bypassing Ras-induced cellular senescence.

Existing studies have demonstrated that cyclin D1 is exported from the nucleus to the cytoplasm. At G1 phase, cyclin D1 complexes with CDK4 and translocates to the nucleus, to phosphorylate Rb following CAK activation. The GSK-3 β kinase then enters the nucleus during G1/S transition and phosphorylates cyclin D1 at Thr286 (5, 38), triggering CRM1-mediated nuclear export of cyclin D1 (39). Once T286-phosphorylated cyclin D1 is exported to the cytoplasm, it is ubiquitinated and degraded by the proteasome (36). In contrast, however, very little is known about the mechanism that regulates cyclin D1's nuclear entry. In our attempts to understand how ASPP2 mediates Ras oncogene-induced senescence, we have identified one mechanism by which cyclin D1's nuclear accumulation is regulated. Cyclin D1 is SUMO-modified by SUMO-2/3 (but not SUMO-1), and ASPP2 inhibits Ras oncogene-induced SUMO modification of endogenous cyclin D1 *in vivo*. Interestingly, SUMO-modified cyclin D1 was nuclear and insoluble, since SUMO-modified cyclin D1 could only be detected when cells were lysed with 8M urea. This may explain why SUMO-modified cyclin D1 has not previously been identified by conventional immunoprecipitation assays or in normal kinase assay lysates. The insoluble nature of SUMO-modified cyclin D1 is in agreement with its nuclear localisation. To detect SUMO-modified endogenous cyclin D1 in Ras-expressing ASPP2 mutant cells, SUMOylated cyclin D1 had to be denatured with 8M urea and the protein refolded in diluted buffer for immunoprecipitation. This refolding process

is likely to only work with a proportion of the population of SUMO-modified cyclin D1, and may be one of the reasons why the mobility shifts of cyclin D1 observed in figures 2C and 3B are similar but not identical. Furthermore, we do not yet know the molecular mechanisms by which ASPP2 prevents Ras oncogene from inducing SUMO modification of cyclin D1.

Previous studies have shown that SUMO-modified proteins tend to locate in the nucleus (40). In some proteins, nuclear accumulation by SUMO modification is achieved by interference with NES (nuclear export signal) functions. By modifying a site in close proximity to a NES, SUMO modification may inhibit nuclear export by masking the NES signal. However, the identified K33 of cyclin D1 is not in close proximity to any known cyclin D1 NES, while the two lysine residues (K95 and K96) in close proximity to the first NES of cyclin D1 failed to influence its nuclear localisation when co-expressed with SUMO-2 and -3. How SUMO modification at K33 can influence the nuclear localisation of cyclin D1, therefore, remains unknown. Future studies are needed to test whether SUMO modification on K33 can mask a NES or expose a nuclear localisation signal (if one exists) of cyclin D1, or whether it causes nuclear retention by facilitating cyclin D1's association with nuclear factors or structures. Regardless of how K33 SUMO modification causes nuclear localisation of cyclin D1, we show here that SUMOylated nuclear cyclin D1 is active in phosphorylating Rb, since the amount of phosphorylated Rb detected in H-RasV12-expressing ASPP2 mutant MEFs is much higher than that in ASPP2 wild type MEFs. This also agrees with the finding that nuclear cyclin D1 is far more potent than the wild type in bypassing Ras oncogene-induced senescence.

Mutation of Ras oncogene and overexpression of cyclin D1 occur frequently in human cancers. In colon and breast cancers for example, mutation of Ras and overexpression of cyclin D1 can be as high as 50% (1, 41, 42). It is also interesting to note that down-regulation of ASPP2 in human breast cancers was also observed in

over 20% of mutant p53 expressing tumours (22). Furthermore, a large percentage of human tumours over-express nuclear cyclin D1, and nuclear localisation is required for the oncogenic properties of cyclin D1. Thus, it will be interesting to identify whether nuclear cyclin D1 expression is associated with Ras mutation and/or a reduced expression of ASPP2. Importantly, inhibiting cyclin D1's SUMO modification may be beneficial in the treatment of patients expressing high levels of nuclear cyclin D1.

Materials and Methods

Cell culture and genotyping

Mouse embryonic fibroblasts (MEFs) were prepared from day 13.5 embryos from XTV-ASPP2^(+/Δ3) intercrosses. Genotyping was performed by PCR using primers a (5'-CCT CTC ACA AAA GGA AAT AAC CTG-3'), b (5'-AGG AAA ACC ACC ACC TTC AC-3'), and c (5'-TAC CCG CTT CCA TTG CTC AG-3'). Primers a and b amplify a 900-bp fragment from the wild type (WT) allele, and primers b and c amplify a 1,100-bp fragment from the knockout allele. p53 MEFs were prepared from day 13.5 embryos from p53 (+/-) intercrosses. All MEFs and U2OS cells were cultured in DMEM supplemented with 10% foetal bovine serum (FBS) and penicillin-streptomycin (Gibco-BRL).

Plasmids

pBabe-Puro Ha-RasV12 and pBabe-Bleo Ha-RasV12 were obtained from Julian Downward. pBabe-Puro cyclin D1 and pBabe-Puro cyclin D1-T286A were obtained

from Alan Diehl. pBabe-Puro cyclin D1-K33A, K72A, K95A and K96A were obtained by site-directed mutagenesis. The following primers were used: K33A (GCG GGC CAT GCT GGC GGC GGA GGA GAC CTG C); K72A (GGT CTG CGA GGA ACA GGC GTG CGA GGA GGA GG); K95A (CGC TGG AGC CCG TGG CAA AGA GCC GCC TGC AGC); K96A (CGC TGG AGC CCG TGA AAG CGA GCC GCC TGC AGC). The retroviral vector for ASPP2 was generated by cloning ASPP2 cDNA fragments into pLPCX-Puro using XhoI and NotI restriction enzymes. 6His-tagged SUMO-1, -2 and -3 were cloned in pcDNA3 using BamHI and EcoRI restriction enzymes.

Western Blot analysis

Western blot (WB) analysis was performed with lysates prepared 6–8 days after transduction of Ras from subconfluent cells, with Urea buffer (8M Urea, 1M Thiourea, 0.5% CHAPS, 50mM DTT, and 24mM Spermine) or NP40 lysis buffer (1%NP40, 0.5% sodium deoxycholate in PBS) as described (43). Primary antibodies were from: Santa Cruz (p21^{waf1/cip1}(F-5), Cyclin E, Cyclin A, cdk2), Abcam (Tubulin, Cyclin D1(DCS-6), p16^{ink4a}, p19^{Arf}), Novocastra (p53(CM-5)), BD Biosciences (Ras, Rb), Upstate (Ras Clone 10), Cell Signaling (Cyclin D1, Cdk4, Ubiquitin), and Invitrogen (SUMO-2/3). Anti-ASPP2 antibodies were generated in rabbits and the serum was named S32. To detect p27kip1 we used the mouse monoclonal SX53.G8. Signals were detected using the ECL detection system (GE Healthcare).

Indirect immunofluorescence

Cells were fixed in 4% PBS-paraformaldehyde for 15 min, incubated in 0.2% Triton-X-100 for 5 min, then in 0.2% Fish Skin Gelatine in PBS for 10 min and stained for 30 min with an anti-Cyclin D1 antibody (Abcam) or anti-His (Santa Cruz) or anti-BrdU FITC (BD bioscience) or anti-p21^{waf1/cip1} (SX118). Antibodies were used at 1:50 dilution in 0.2% Fish Skin Gelatine-PBS. Staining with the secondary antibody was performed as previously described (44), followed by visualization under a fluorescence microscope. All the procedure was performed at the temperature of 20 degrees.

Analysis of senescence

Analysis of senescence in cell culture was performed using a Senescence β -galactosidase staining kit (Cell Signaling) as described previously (43). To quantify SA- β -gal positives, at least 200 cells were counted in random fields in each of the duplicated wells.

Transformation assays

10^5 ASPP2^($\Delta 3/\Delta 3$) and ASPP2^(+/+) MEFs were infected with pBABE-Puro H-RasV12 or empty vector retroviruses. Cells were selected with puromycin for 4 days, and plates then fixed and stained with Giemsa 4 weeks later. For anchorage-independent growth, 5×10^4 cells transduced with pBABE-Puro H-RasV12 were resuspended in medium containing 0.3% low-melting-point agarose and plated onto solidified bottom layer medium containing 0.5% agarose. Colonies were photographed and counted after 3–4 weeks.

Immunoprecipitations

Cells were lysed in Urea buffer (8M Urea, 1M Thiourea, 0.5% CHAPS, 50mM DTT, and 24mM Spermine), after which, extracts were diluted 10-fold in NP40 lysis buffer (1%NP40, 0.5% sodium deoxycholate in PBS) and precleared with 60 μ l of protein G beads (50% slurry) for 60 min at 4°C. For each immunoprecipitation, 25 μ l anti-cyclin D1 mAb (Abcam) or IgG was used, 25 μ l of 50% slurry of protein G beads were added, and then samples rotated at 4°C overnight. Beads were washed five times with 1 ml of 10-fold diluted Urea buffer, and 20 μ l of 2 \times SDS loading buffer added. Immunoprecipitations were analysed by WB as indicated.

Purification of 6His-tagged SUMO-cyclin D1 conjugates

36 h post transfection, cells were washed twice with PBS and scraped in 1 ml of PBS. 20% of the cell suspension was used for direct Western blot analysis. The remainder was lysed in 6 ml of 6 M guanidinium-HCl, 0.1 M Na₂HPO₄/NaH₂PO₄, 0.01 M Tris/HCl, pH 8.0, 5 mM imidazole and 10 mM β -mercaptoethanol. 75 μ l of Ni²⁺-NTA-agarose beads (Qiagen) was then added and lysates rotated at 20°C for 4 h. The beads were successively washed for 5 min in each step at 20°C with 750 μ l of each of the following buffers: 6 M guanidinium-HCl, 0.1 M Na₂HPO₄/NaH₂PO₄, 0.01 M Tris/HCl, pH 8.0, 10 mM β -mercaptoethanol; 8 M urea, 0.1 M Na₂HPO₄/NaH₂PO₄, 0.01 M Tris/HCl, pH8.0, 10 mM β -mercaptoethanol; 8 M urea, 0.1 M Na₂HPO₄/NaH₂PO₄, 0.01 M Tris/HCl, pH 6.3, 10 mM β -mercaptoethanol (buffer A) plus 0.2% Triton X-100; buffer A and then buffer A plus 0.1% Triton X-100. After the last wash, 6His-tagged SUMOylated products were eluted by incubating beads in 75 μ l of 200 mM imidazole, 0.15 M Tris/HCl pH6.7, 30% glycerol, 0.72 M β -

mercaptoethanol, 5% SDS for 20 min at 20°C. Eluates were mixed at a 1:1 ratio with 2x Laemmli-buffer and analysed by WB.

Acknowledgements

We would like to thank the Ludwig Institute for Cancer Research, EU and AICR for supporting this work and Dr Claire Beveridge for her help in preparing the manuscript. EL was partially supported by a FIRC fellowship.

1. Barnes DM, Gillett CE. Cyclin D1 in breast cancer. *Breast cancer research and treatment* 1998; 52(1-3): 1-15.
2. Shamma A, Doki Y, Shiozaki H, Tsujinaka T, Yamamoto M, Inoue M, *et al.* Cyclin D1 overexpression in esophageal dysplasia: a possible biomarker for carcinogenesis of esophageal squamous cell carcinoma. *International journal of oncology* 2000 Feb; 16(2): 261-266.
3. Quelle DE, Ashmun RA, Shurtleff SA, Kato JY, Bar-Sagi D, Roussel MF, *et al.* Overexpression of mouse D-type cyclins accelerates G1 phase in rodent fibroblasts. *Genes & development* 1993 Aug; 7(8): 1559-1571.
4. Resnitzky D, Gossen M, Bujard H, Reed SI. Acceleration of the G1/S phase transition by expression of cyclins D1 and E with an inducible system. *Molecular and cellular biology* 1994 Mar; 14(3): 1669-1679.
5. Diehl JA, Cheng M, Roussel MF, Sherr CJ. Glycogen synthase kinase-3beta regulates cyclin D1 proteolysis and subcellular localization. *Genes & development* 1998 Nov 15; 12(22): 3499-3511.
6. Alt JR, Cleveland JL, Hannink M, Diehl JA. Phosphorylation-dependent regulation of cyclin D1 nuclear export and cyclin D1-dependent cellular transformation. *Genes & development* 2000 Dec 15; 14(24): 3102-3114.
7. Gladden AB, Woolery R, Aggarwal P, Wasik MA, Diehl JA. Expression of constitutively nuclear cyclin D1 in murine lymphocytes induces B-cell lymphoma. *Oncogene* 2006 Feb 16; 25(7): 998-1007.
8. Lin DI, Lessie MD, Gladden AB, Bassing CH, Wagner KU, Diehl JA. Disruption of cyclin D1 nuclear export and proteolysis accelerates mammary carcinogenesis. *Oncogene* 2008 Feb 21; 27(9): 1231-1242.
9. Johnson ES. Protein modification by SUMO. *Annual review of biochemistry* 2004; 73: 355-382.
10. Vertegaal AC, Andersen JS, Ogg SC, Hay RT, Mann M, Lamond AI. Distinct and overlapping sets of SUMO-1 and SUMO-2 target proteins revealed by quantitative proteomics. *Mol Cell Proteomics* 2006 Dec; 5(12): 2298-2310.
11. Saitoh H, Hinchey J. Functional heterogeneity of small ubiquitin-related protein modifiers SUMO-1 versus SUMO-2/3. *The Journal of biological chemistry* 2000 Mar 3; 275(9): 6252-6258.
12. Bylebyl GR, Belichenko I, Johnson ES. The SUMO isopeptidase Ulp2 prevents accumulation of SUMO chains in yeast. *The Journal of biological chemistry* 2003 Nov 7; 278(45): 44113-44120.
13. Tatham MH, Jaffray E, Vaughan OA, Desterro JM, Botting CH, Naismith JH, *et al.* Polymeric chains of SUMO-2 and SUMO-3 are

- conjugated to protein substrates by SAE1/SAE2 and Ubc9. *The Journal of biological chemistry* 2001 Sep 21; 276(38): 35368-35374.
14. Matic I, van Hagen M, Schimmel J, Macek B, Ogg SC, Tatham MH, *et al.* In vivo identification of human small ubiquitin-like modifier polymerization sites by high accuracy mass spectrometry and an in vitro to in vivo strategy. *Mol Cell Proteomics* 2008 Jan; 7(1): 132-144.
 15. Anckar J, Sistonen L. SUMO: getting it on. *Biochemical Society transactions* 2007 Dec; 35(Pt 6): 1409-1413.
 16. Lloyd AC. Ras versus cyclin-dependent kinase inhibitors. *Curr Opin Genet Dev* 1998 Feb; 8(1): 43-48.
 17. Weber JD, Taylor LJ, Roussel MF, Sherr CJ, Bar-Sagi D. Nucleolar Arf sequesters Mdm2 and activates p53. *Nature Cell Biology* 1999; 1(May 1999): 20-26.
 18. Pantoja C, Serrano M. Murine fibroblasts lacking p21 undergo senescence and are resistant to transformation by oncogenic Ras. *Oncogene* 1999 Sep 2; 18(35): 4974-4982.
 19. Serrano M, Lin AW, McCurrach ME, Beach D, Lowe SW. Oncogenic ras provokes premature cell senescence associated with accumulation of p53 and p16INK4a. *Cell* 1997 Mar 7; 88(5): 593-602.
 20. Sebastian T, Malik R, Thomas S, Sage J, Johnson PF. C/EBPbeta cooperates with RB:E2F to implement Ras(V12)-induced cellular senescence. *The EMBO journal* 2005 Sep 21; 24(18): 3301-3312.
 21. Guo X, Keyes WM, Papazoglu C, Zuber J, Li W, Lowe SW, *et al.* TAp63 induces senescence and suppresses tumorigenesis in vivo. *Nature cell biology* 2009 Dec; 11(12): 1451-1457.
 22. Samuels-Lev Y, O'Connor DJ, Bergamaschi D, Trigianti G, Hsieh JK, Zhong S, *et al.* ASPP proteins specifically stimulate the apoptotic function of p53. *Mol Cell* 2001 Oct; 8(4): 781-794.
 23. Vives V, Su J, Zhong S, Ratnayaka I, Slee E, Goldin R, *et al.* ASPP2 is a haploinsufficient tumor suppressor that cooperates with p53 to suppress tumor growth. *Genes & development* 2006 May 15; 20(10): 1262-1267.
 24. Kampa KM, Acoba JD, Chen D, Gay J, Lee H, Beemer K, *et al.* Apoptosis-stimulating protein of p53 (ASPP2) heterozygous mice are tumor-prone and have attenuated cellular damage-response thresholds. *Proceedings of the National Academy of Sciences of the United States of America* 2009 Mar 17; 106(11): 4390-4395.
 25. Liu ZJ, Lu X, Zhang Y, Zhong S, Gu SZ, Zhang XB, *et al.* Downregulated mRNA expression of ASPP and the hypermethylation of the 5'-

untranslated region in cancer cell lines retaining wild-type p53. *FEBS letters* 2005 Mar 14; 579(7): 1587-1590.

26. Lossos IS, Natkunam Y, Levy R, Lopez CD. Apoptosis stimulating protein of p53 (ASPP2) expression differs in diffuse large B-cell and follicular center lymphoma: correlation with clinical outcome. *Leukemia & lymphoma* 2002 Dec; 43(12): 2309-2317.
27. Yang JP, Hori M, Takahashi N, Kawabe T, Kato H, Okamoto T. NF-kappaB subunit p65 binds to 53BP2 and inhibits cell death induced by 53BP2. *Oncogene* 1999 Sep 16; 18(37): 5177-5186.
28. Naumovski L, Cleary ML. The p53-binding protein 53BP2 also interacts with Bc12 and impedes cell cycle progression at G2/M. *Molecular and cellular biology* 1996 Jul; 16(7): 3884-3892.
29. Egloff MP, Johnson DF, Moorhead G, Cohen PT, Cohen P, Barford D. Structural basis for the recognition of regulatory subunits by the catalytic subunit of protein phosphatase 1. *The EMBO journal* 1997 Apr 15; 16(8): 1876-1887.
30. Espanel X, Sudol M. Yes-associated protein and p53-binding protein-2 interact through their WW and SH3 domains. *The Journal of biological chemistry* 2001 Apr 27; 276(17): 14514-14523.
31. Nakagawa H, Koyama K, Murata Y, Morito M, Akiyama T, Nakamura Y. APCL, a central nervous system-specific homologue of adenomatous polyposis coli tumor suppressor, binds to p53-binding protein 2 and translocates it to the perinucleus. *Cancer research* 2000 Jan 1; 60(1): 101-105.
32. Chen Y, Liu W, McPhie DL, Hassinger L, Neve RL. APP-BP1 mediates APP-induced apoptosis and DNA synthesis and is increased in Alzheimer's disease brain. *The Journal of cell biology* 2003 Oct 13; 163(1): 27-33.
33. Barbash O, Zamfirova P, Lin DI, Chen X, Yang K, Nakagawa H, *et al.* Mutations in Fbx4 inhibit dimerization of the SCF(Fbx4) ligase and contribute to cyclin D1 overexpression in human cancer. *Cancer cell* 2008 Jul 8; 14(1): 68-78.
34. Okabe H, Lee SH, Phuchareon J, Albertson DG, McCormick F, Tetsu O. A critical role for FBXW8 and MAPK in cyclin D1 degradation and cancer cell proliferation. *PloS one* 2006; 1: e128.
35. Xue Y, Zhou F, Fu C, Xu Y, Yao X. SUMOsp: a web server for sumoylation site prediction. *Nucleic acids research* 2006 Jul 1; 34(Web Server issue): W254-257.

36. Lin DI, Barbash O, Kumar KG, Weber JD, Harper JW, Klein-Szanto AJ, *et al.* Phosphorylation-dependent ubiquitination of cyclin D1 by the SCF(FBX4-alphaB crystallin) complex. *Molecular cell* 2006 Nov 3; 24(3): 355-366.
37. Liu JJ, Chao JR, Jiang MC, Ng SY, Yen JJ, Yang-Yen HF. Ras transformation results in an elevated level of cyclin D1 and acceleration of G1 progression in NIH 3T3 cells. *Molecular and cellular biology* 1995 Jul; 15(7): 3654-3663.
38. Diehl JA, Zindy F, Sherr CJ. Inhibition of cyclin D1 phosphorylation on threonine-286 prevents its rapid degradation via the ubiquitin-proteasome pathway. *Genes & development* 1997 Apr 15; 11(8): 957-972.
39. Benzeno S, Diehl JA. C-terminal sequences direct cyclin D1-CRM1 binding. *The Journal of biological chemistry* 2004 Dec 31; 279(53): 56061-56066.
40. Rodriguez MS, Dargemont C, Hay RT. SUMO-1 conjugation in vivo requires both a consensus modification motif and nuclear targeting. *The Journal of biological chemistry* 2001 Apr 20; 276(16): 12654-12659.
41. Downward J. Targeting RAS signalling pathways in cancer therapy. *Nature reviews* 2003 Jan; 3(1): 11-22.
42. Bartkova J, Lukas J, Muller H, Lutzhoft D, Strauss M, Bartek J. Cyclin D1 protein expression and function in human breast cancer. *International journal of cancer* 1994 May 1; 57(3): 353-361.
43. Wang W, Chen JX, Liao R, Deng Q, Zhou JJ, Huang S, *et al.* Sequential activation of the MEK-extracellular signal-regulated kinase and MKK3/6-p38 mitogen-activated protein kinase pathways mediates oncogenic ras-induced premature senescence. *Mol Cell Biol* 2002 May; 22(10): 3389-3403.
44. Slee EA, Gillotin S, Bergamaschi D, Royer C, Llanos S, Ali S, *et al.* The N-terminus of a novel isoform of human iASPP is required for its cytoplasmic localization. *Oncogene* 2004 Dec 2; 23(56): 9007-9016.

Figure Legends

Figure 1

ASPP2 mediates senescence induced by H-RasV12

Mouse embryonic fibroblasts (MEFs) generated from ASPP2^(+/+) and ASPP2^(Δ3/Δ3) embryos were infected with oncogenic H-RasV12 and stained for senescence associated β-galactosidase (SA-β-gal) activity (A). Comparison of the number of colonies formed by ASPP2^(+/+) and ASPP2^(Δ3/Δ3) MEFs transduced with empty vector (Vector) or H-RasV12 (Ras) expressing retroviruses (B). Anchorage-independent growth assay for ASPP2^(+/+) and ASPP2^(Δ3/Δ3) MEFs transduced with H-RasV12 (C). Colonies were photographed at 20x magnification. Error bars represent SD of at least 3 independent experiments.

H-RasV12 expressing ASPP2^(Δ3/Δ3) MEFs were infected with retroviruses expressing full length ASPP2 or empty vector and subjected to SA-β-gal staining. The percentage of SA-β-gal positive cells is shown in the right panel. Error bars represent the range from 2 independent experiments (D).

Figure 2

ASPP2 inhibits Rb phosphorylation and nuclear accumulation of cyclin D1 induced by Ras oncogene independently of p53

WBs showing the expression levels of: endogenous ASPP2, p19^{Arf}, p53 and p21^{waf1/cip1} as indicated in ASPP2^(+/+) and ASPP2^(Δ3/Δ3) MEFs, with or without H-

RasV12 expression (A); phosphorylated Rb and total Rb (B); and cyclin D1, cdk4, p16^{ink4a}, p27kip1, cyclin A, cyclin E and cdk2 in ASPP2^(+/+) and ASPP2^(Δ3/Δ3) MEFs, with or without H-RasV12 expression (C). In B, the ratio of p-Rb to Rb was calculated by densitometry using QuantityOne software and error bars represent the range from 2 independent experiments. (D) Expression levels of p53, p19^{Arf}, p21^{waf1/cip1} and cyclin D1 in p53^(+/+) and p53^(-/-) MEFs with or without H-RasV12 expression. Tubulin expression levels confirm equal loading. (E) Indirect immunofluorescence of cyclin D1 in ASPP2^(+/+) or ASPP2^(Δ3/Δ3) MEFs, and p53^(+/+) or p53^(-/-) MEFs, with or without H-RasV12 expression. Graphs show the percentage of nuclear cyclin D1 expressing cells. Error bars represent the range from 2 independent experiments.

Figure 3

H-RasV12 induces accumulation of SUMO-modified cyclin D1 in ASPP2^(Δ3/Δ3) MEFs

- A. H-RasV12 expression does not affect cyclin D1's ubiquitination pattern. Total cell lysates (6 mg) derived from ASPP2^(-/-) MEFs with or without H-RasV12 expression, treated with proteasomal inhibitor MG132 where indicated, were immunoprecipitated with anti-cyclin D1 or control (IgG) antibodies. Immunoprecipitates and an aliquot (50 μg) of total cell lysate were subjected to WB analysis using anti-ubiquitin antibody. Ubiquitin-cyclin D1 is labeled.
- B. Total cell lysates (6 mg) derived from ASPP2^(Δ3/Δ3) MEFs, with or without H-RasV12 expression, were immunoprecipitated and subjected to WB analysis as in (A) to detect SUMO-modified cyclin D1 as labelled.

C. ASPP2^(Δ3/Δ3) MEFs, with or without H-RasV12 expression, were transfected with 1 μg of cyclin D1-expressing plasmid, with or without 1 μg of plasmid expressing 6His-tagged SUMO-1 or 6His-tagged SUMO-2 and 6His-tagged SUMO-3. 6His-tagged SUMOs were trapped on a nickel column, and SUMOylated products separated and analysed with anti-cyclin D1 antibody to detect SUMO-modified cyclin D1 as indicated.

Figure 4

SUMO modification leads to nuclear accumulation of cyclin D1

- A. Indirect immunofluorescence of cyclin D1 and SUMO in U2OS cells co-transfected with cyclin D1, SUMO-1, or SUMO-2 and SUMO-3 expressing plasmids. Graphs show the percentage of nuclear cyclin D1 expressing cells over the total number of cyclin D1 expressing cells. Error bars represent the range from 3 independent experiments.
- B. Indirect immunofluorescence showing expression of endogenous cyclin D1 in H-RasV12 expressing ASPP2^(Δ3/Δ3) MEFs, infected with control or SENP2 expressing adenovirus for 24 hours. The percentage of nuclear cyclin D1 expressing cells is indicated in the bottom/right corner of each panel.

Figure 5

K33 is critical for cyclin D1's nuclear localisation

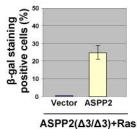
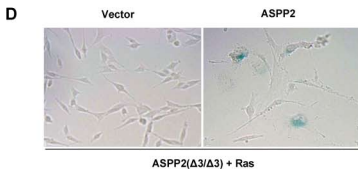
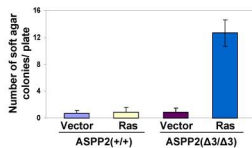
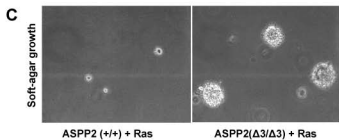
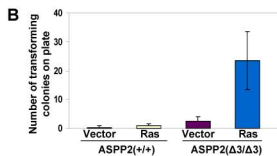
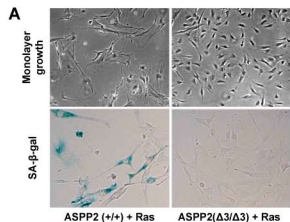
- A. Cyclin D1 protein sequence with SUMOylation sites highlighted (with Lysine residues in blue and flanking residues in red).

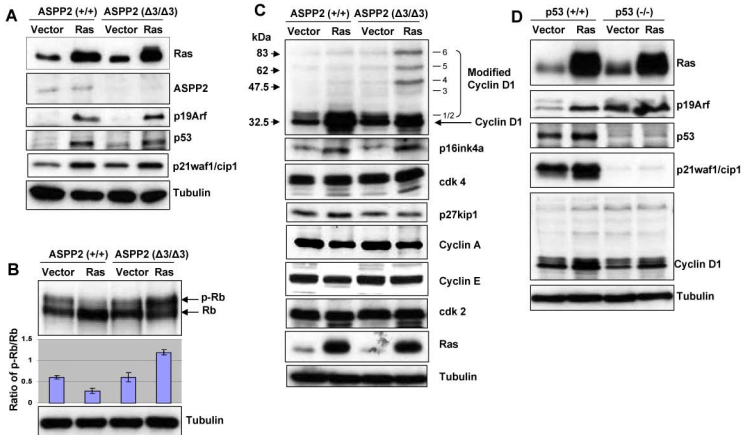
B. Indirect immunofluorescence of cyclin D1 and SUMO-2/3 in U2OS cells co-transfected with cyclin D1, cyclin D1 puntiform mutants and SUMO-2 and SUMO-3 expressing plasmids. Graphs show the percentage of nuclear cyclin D1 expressing cells over the total number of cyclin D1 expressing cells. Error bars represent the range from 3 independent experiments.

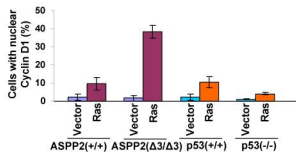
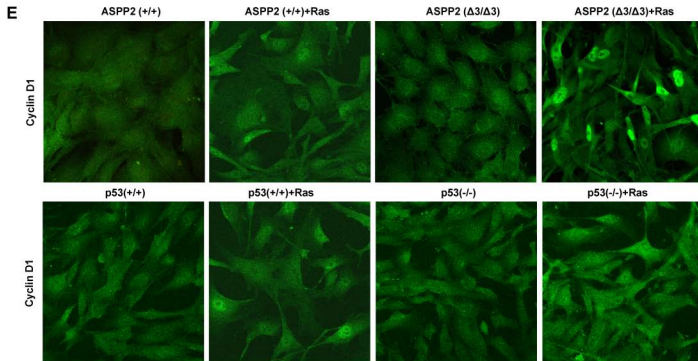
Figure 6

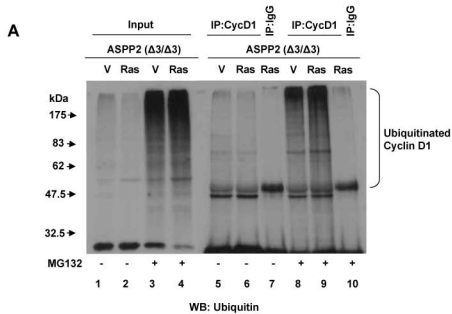
Overexpression of the constitutively nuclear cyclin D1 mutant is sufficient to overcome Ras-induced senescence

WB (A) and indirect immunofluorescence (B) showing expression of exogenous (Ex) and endogenous (End) cyclin D1 and Ras in ASPP2^(+/+) MEFs, infected with control, cyclin D1 or cyclin D1-T286A expressing retrovirus, with or without H-RasV12 expressing retrovirus. ASPP2^(+/+) MEFs infected as in A were stained for senescence-associated β -galactosidase (SA- β -gal) activity (C) and BrdU incorporation (D), after 24h pulse, 1 week after infection. Graphs show the percentage of SA- β -gal positive cells over the total number cells (E) and the percentage of BrdU positive cells over the total number of cells (F). Error bars represent the range from 3 independent experiments.

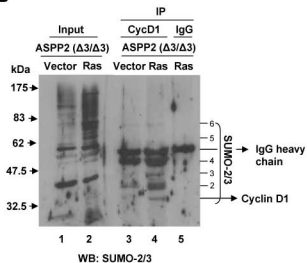




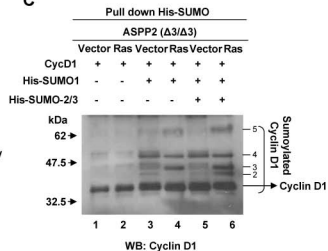


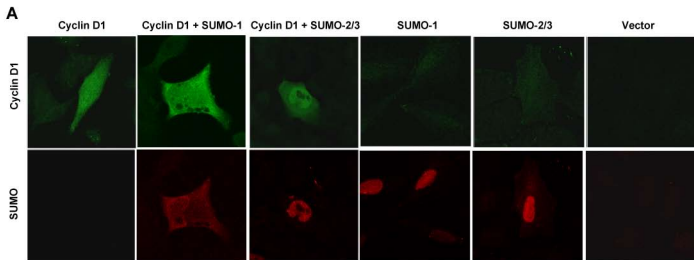


B

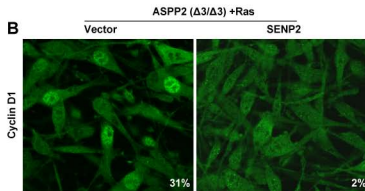
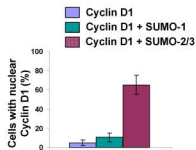


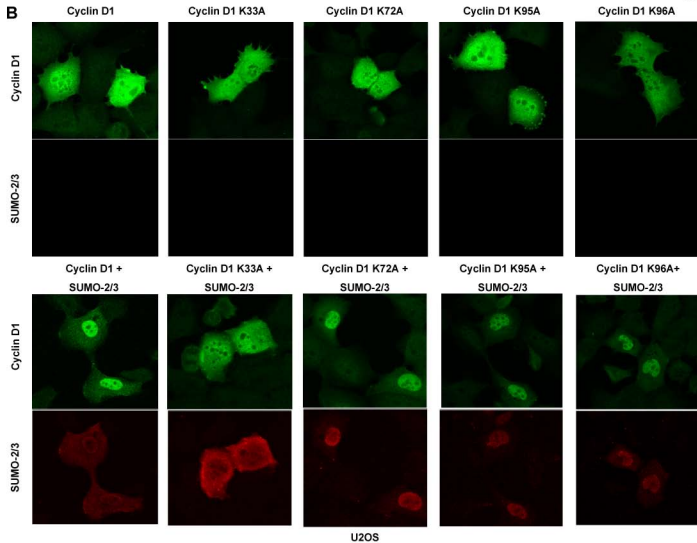
C





U2OS





A

1	MEHQLLCCEVETIRRAYPDTNLLNDRVLR	AMLKTEETCAPSVSYFKCVQK	50
51	EIVPSMRKIVATWMLVCE	EEQKEEEVFPLAMNYLDRFLSLEPLKKSRLQ	100
101	LLGATCMFVASKMKETIPLTAEKLCIYTDNSIRPEELLQMELLLLVNKLKW		150
151	NLAAMTPHDFIEHFLSKMPEADENKQTIRKHAQTFVALCATDVKFI	SNPP	200
201	SMVAAGSVVAAMQGLNLGSPNNFLSCYRTHFLSRVIKCDPDCLRACQEQ		250
251	IEALLESSLRQAQQNVDPKATEEEGEVEEEAGLACTPTDVRD	VDI	295

B

